IOSR Journal of Applied Physics (IOSR-JAP)
e-ISSN: 2278-4861.Volume 17, Issue 2 Ser. 1 (Mar. – Apr. 2025), PP 20-27
www.iosrjournals.org

Spectral, Transmittance and Upconversion Properties of Pr^{3+} Doped Bismuth Borate Glasses

S.L.Meena
Ceramic Laboratory, Department of physics, Jai Narain Vyas University, Jodhpur 342001(Raj.) Ind
E-mail address:shankardiya7@rediffmail.com

Abstract
Zinc lithium calcium magnesium tantalum bismuth borate glasses containing Pr^{3+} in (35-x):Bi_2O_3:10ZnO:10Li_2O:10CaO:10MgO:10Ta_2O_5:15B_2O_3:xPr_2O_3 (where x=1, 1.5,2 mol %) have been prepared by melt-quenching method. The amorphous nature of the glasses was confirmed by x-ray diffraction studies. Transmittance Optical absorption, Excitation and fluorescence spectra were recorded at room temperature for all glass samples. Judd-Ofelt intensity parameters Ω_λ (λ=2, 4, 6) are evaluated from the intensities of various absorption bands of optical absorption spectra. Using these intensity parameters various radiative properties like spontaneous emission probability, branching ratio, radiative life time and stimulated emission cross–section of various emission lines have been evaluated.

Keywords: *ZLCMTBB Glasses, Optical Properties, Intensity parameters, Transmittance and Upconversion Properties Introduction*

Date of Submission: 05-03-2025 Date of Acceptance: 17-03-2025

I. Introduction

Rare earth glasses have attracted much attention, because they have large potential applications in many fields, such as electro-luminescent devices, memory devices sensors, glass lasers, optical fiber amplifiers, up-conversion lasers and flat-panel displays [1–5].Among different glasses, borate glasses have unique properties. They have high transparency, high refractive index and low dispersion rates [6-8].

Bismuth borate glasses possess interesting properties high density, high solubility, non-linear optical susceptibilities and low melting temperature [9-12].Due to their excellent thermal, physical and mechanical properties, they are used in fiber lasers, thermal imaging, spectral conversion, photo-voltaic solar cells, temperature sensors and optical coherence tomography [13-15].The addition of network modifier (NWF) Li_2O is to improve both electrical and mechanical properties of such glasses. Recently, rare earth doped borate glass has attracted much interest because of high rare earth ion solubility, optical data transmission, detection, sensor and catalysts [16, 17].

In this work, the spectroscopic properties of Pr^{3+} -doped (35-x):Bi_2O_3:10ZnO:10Li_2O:10CaO:10MgO:10Ta_2O_5:15B_2O_3:Pr_2O_3 (where x=1, 1.5,2 mol %) glasses were investigated. The Transmittance, absorption, Excitation and fluorescence spectra of Pr^{3+} of the glasses were investigated. The J-O intensity parameters render significant information regarding local structure and bonding in the vicinity of rare- earth ions.

II. Experimental Techniques

Preparation of glasses

The following Pr^{3+} doped zinc lithium calcium magnesium tantalum bismuth borate glass samples (35-x): Bi_2O_3: 10ZnO: 10Li_2O: 10CaO: 10MgO: 10Ta_2O_3: 15B_2O_3:Pr_2O_3 (where x=1, 1.5.2) have been prepared by melt-quenching method. Analytical reagent grade chemical used in the present study consist of Bi_2O_3, ZnO, Li_2O,CaO,MgO, Ta_2O_3,$B_2O_3$and Pr_2O_3. All weighed chemicals were powdered by using an Agate pestle mortar and mixed thoroughly before each batch (10g) was melted in alumina crucibles in silicon carbide based an electrical furnace.

Silicon Carbide Muffle furnace was heated to working temperature of 960^0C, for preparation of Zinc lithium calcium magnesium tantalum bismuth borate glasses, for two hours to ensure the melt to be free from gases. The melt was stirred several times to ensure homogeneity. For quenching, the melt was quickly poured on the steel plate & was immediately inserted in the muffle furnace for annealing. The steel plate was preheated to100^0C.While pouring; the temperature of crucible was also maintained to prevent crystallization. And

annealed at temperature of 250^0C for 2h to remove thermal strains and stresses. Every time fine powder of cerium oxide was used for polishing the samples. The glass samples so prepared were of good optical quality and were transparent. The chemical compositions of the glasses with the name of samples are summarized in Table 1

Table 1 Chemical composition of the glasses

Sample	Glass composition (mol %)
ZLCMTBB (UD)	$35Bi_2O_3$:10ZnO:10Li_2O:10CaO:10MgO:10Ta_2O_5:15B_2O
ZLCMTBB(PR 1)	$34Bi_2O_3$:10ZnO:10Li_2O:10CaO:10MgO:10Ta_2O_5:15B_2O_3:1 Pr_2O_3
ZLCMTBB(PR1.5)	$33.5Bi_2O_3$:10ZnO:10Li_2O:10CaO:10MgO:10Ta_2O_5:15B_2O_3:1.5Pr_2O_3
ZLCMTBB(PR 2)	$33Bi_2O_3$:10ZnO:10Li_2O:10CaO:10MgO:10Ta_2O_5:15B_2O_3: 2 Pr_2O_3

ZLCMTBB (UD)—Represents undoped Zinc Lithium Calcium Magnesium Tantalum Bismuth Borate glass specimen.
ZLCMTBB (PR) -Represents Pr^{3+} Zinc Lithium Calcium Magnesium Tantalum Bismuth Borate glass specimens.

III. THEORY

3.1 Oscillator Strength

The intensity of spectral lines are expressed in terms of oscillator strengths using the relation [18].

$$f_{expt.} = 4.318 \times 10^{-9} \int \varepsilon(\nu)\, d\nu \qquad (1)$$

where, $\varepsilon(\nu)$ is molar absorption coefficient at a given energy ν (cm^{-1}), to be evaluated from Beer–Lambert law. Under Gaussian Approximation, using Beer–Lambert law, the observed oscillator strengths of the absorption bands have been experimentally calculated, using the modified relation [19].

$$P_m = 4.6 \times 10^{-9} \times \frac{1}{cl} \log \frac{I_0}{I} \times \Delta\upsilon_{1/2} \qquad (2)$$

where c is the molar concentration of the absorbing ion per unit volume, I is the optical path length, $\log I_0/I$ is absorbtivity or optical density and $\Delta\upsilon_{1/2}$ is half band width.

3.2. Judd-Ofelt Intensity Parameters

According to Judd [20] and Ofelt [21] theory, independently derived expression for the oscillator strength of the induced forced electric dipole transitions between an initial J manifold $|4f^N (S, L) J\rangle$ level and the terminal J' manifold $|4f^N (S',L') J'\rangle$ is given by:

$$\frac{8\Pi^2 mc\bar{\upsilon}}{3h(2J+1)} \frac{1}{n}\left[\frac{(n^2+2)^2}{9}\right] \times S(J, J') \qquad (3)$$

where, the line strength S (J, J') is given by the equation

$$S(J, J') = e^2 \sum_{\lambda=2,4,6} \Omega_\lambda \langle 4f^N (S, L) J \| U^{(\lambda)} \| 4f^N (S', L') J' \rangle^2 \qquad (4)$$

In the above equation m is the mass of an electron, c is the velocity of light, ν is the wave number of the transition, h is Planck's constant, n is the refractive index, J and J' are the total angular momentum of the initial and final level respectively, Ω_λ (λ = 2, 4 and 6) are known as Judd-Ofelt intensity parameters.

3.3.Radiative Properties

The Ω_λ parameters obtained using the absorption spectral results have been used to predict radiative properties such as spontaneous emission probability (A) and radiative life time (τ_R), and laser parameters like fluorescence branching ratio (β_R) and stimulated emission cross section (σ_p).

The spontaneous emission probability from initial manifold $|4f^N (S', L') J'\rangle$ to a final manifold $|4f^N (S, L) J\rangle$ is given by:

$$A[(S', L') J'; (S, L) J] = \frac{64\pi^4 \nu^3}{3h(2J'+1)} \left[\frac{n(n^2+2)^2}{9}\right] \times S(J', \bar{J}) \qquad (5)$$

Where, $S(J', J) = e^2 [\Omega_2 \| U^{(2)} \|^2 + \Omega_4 \| U^{(4)} \|^2 + \Omega_6 \| U^{(6)} \|^2]$

The fluorescence branching ratio for the transitions originating from a specific initial manifold $|4f^N (S', L') J'\rangle$ to a final many fold $|4f^N (S, L) J\rangle$ is given by

$$\beta[(S', L') J'; (S, L) J] = \sum_{S\,L\,J} \frac{A[(S' L') J' (S L) J]}{A[(S' L') J' (S L) J]} \qquad (6)$$

where, the sum is over all terminal manifolds.

The radiative life time is given by

$$\tau_{rad} = \sum_{S\ L\ J} A[(S', L')\ J'; (S,L)\ ] = A_{Total}^{-1} \qquad (7)$$

where, the sum is over all possible terminal manifolds. The stimulated emission cross -section for a transition from an initial manifold $|4f^N (S', L')\ J'>$ to a final manifold $|4f^N (S, L)\ J>|$ is expressed as

$$\sigma_p(\lambda_p) = \left[\frac{\lambda_p^4}{8\pi c n^2 \Delta\lambda_{eff}}\right] \times A[(S', L')\ J'; (\bar{S}, \bar{L})\bar{J}] \qquad (8)$$

where, λ_p the peak fluorescence wavelength of the emission band and $\Delta\lambda_{eff}$ is the effective fluorescence line width.

3.4 Nephelauxetic Ratio (β) and Bonding Parameter ($b^{1/2}$)

The nature of the R-O bond is known by the Nephelauxetic Ratio (β') and Bonding Parameters ($b^{1/2}$), which are computed by using following formulae [22, 23]. The Nephelauxetic Ratio is given by

$$\beta' = \frac{\nu_g}{\nu_a} \qquad (9)$$

where, ν_a and ν_g refer to the energies of the corresponding transition in the glass and free ion, respectively. The values of bonding parameter $b^{1/2}$ are given by

$$b^{1/2} = \left[\frac{1-\beta'}{2}\right]^{1/2} \qquad (10)$$

IV. Result and Discussion

4.1 XRD Measurement

Figure 1 presents the XRD pattern of the samples containing show no sharp Bragg's peak, but only a broad diffuse hump around low angle region. This is the clear indication of amorphous nature with in the resolution limit of XRD instrument.

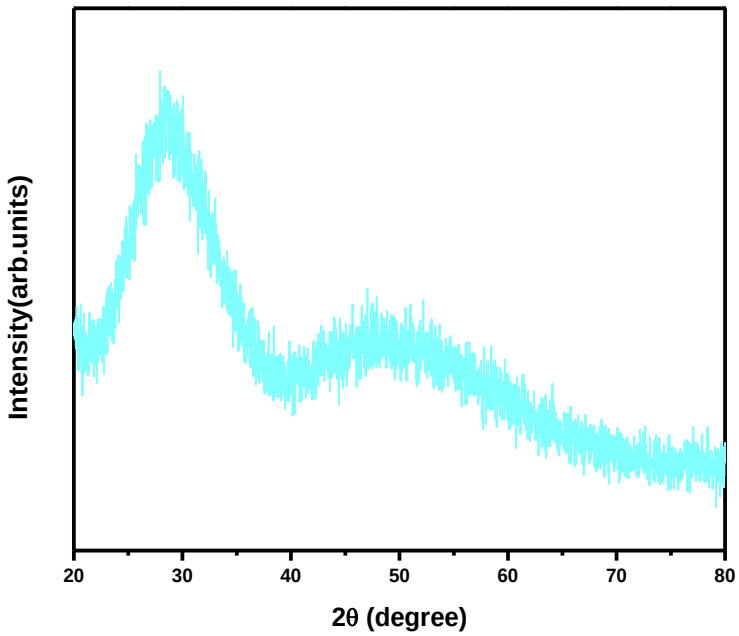

Fig.1: X-ray diffraction pattern of ZLCMTBB PR (01) glass.

4.2 Transmittance Spectra

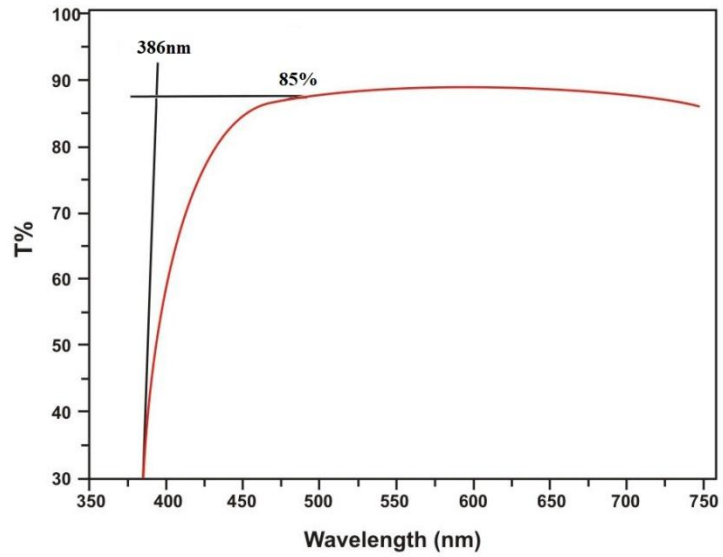

Fig.2:Transmittance Spectra of ZLCMTBB PR (01) glass.

4.3 Up conversion Emission Mechanism

Up-conversion emission mechanism for the Zinc lithium calcium magnesium tantalum bismuth borate glasses are schematically depicted as fig.3

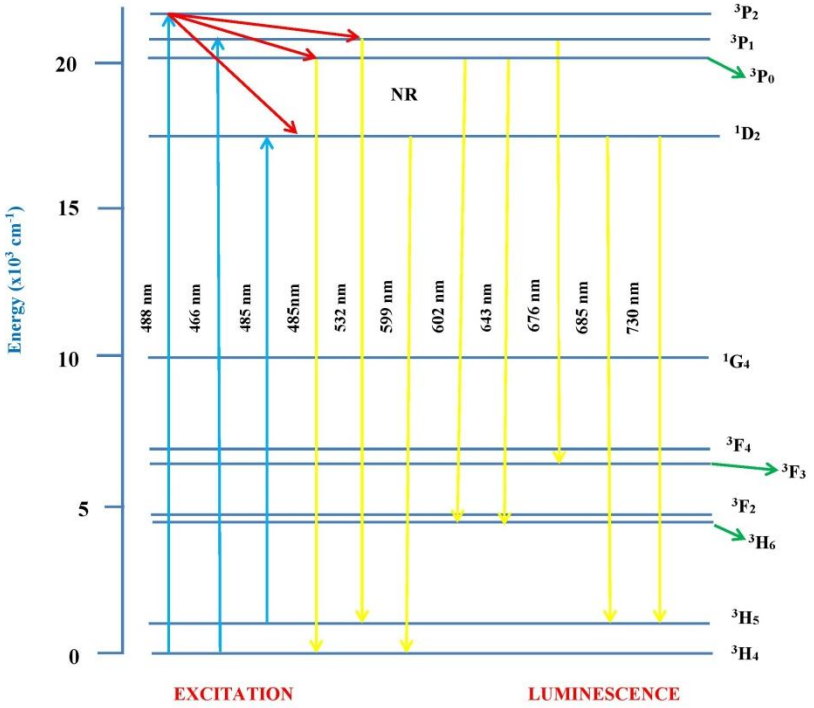

Fig.3 : Upconversion emission Mechanism.

4.4 Absorption spectra

The absorption spectra of ZLCMTBB PR (01) glass, consists of absorption bands corresponding to the absorptions from the ground state $^3H_4$ of Pr^{3+} ions. Eight absorption bands have been observed from the ground state $^3H_4$ to excited states $^3F_2$, $^3F_3$, $^3F_4$, $^1G_4$, $^1D_2$, $^3P_0$, $^3P_1$ and $^3P_2$ for Pr^{3+} doped ZLCMTBB PR (01)glass.

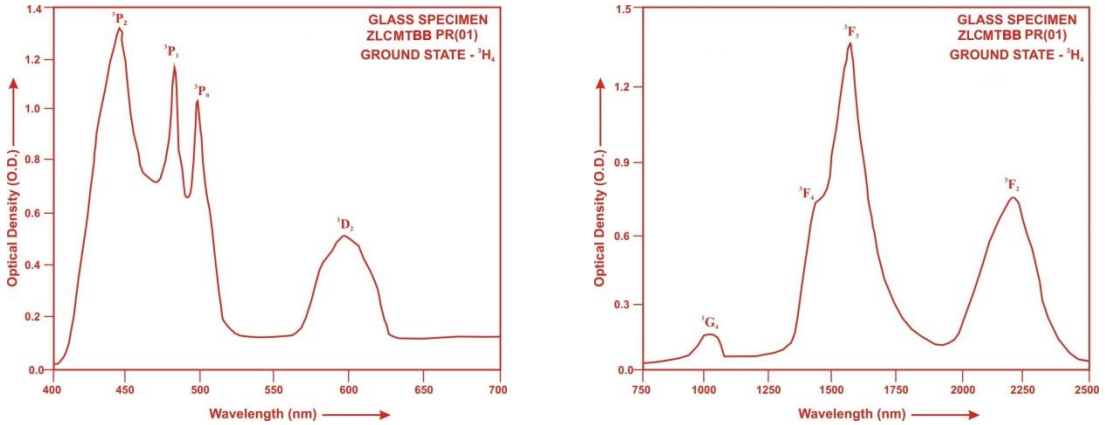

Fig.4: Absorption spectra of ZLCMTBB PR (01) glass.

The experimental and calculated oscillator strengths for Pr^{3+} ions in Zinc lithium calcium magnesium tantalum bismuth borate glasses are given in **Table 2**

Table 2. Measured and calculated oscillator strength ($P^m \times 10^{+6}$) of Pr^{3+} ions in ZLCMTBB glasses.

Energy level $^3H_4$	Glass ZLCMTBB (PR01)		Glass ZLCMTBB (PR1.5)		Glass ZLCMTBB (PR02)	
	$P_{exp.}$	$P_{cal.}$	$P_{exp.}$	$P_{cal.}$	$P_{exp.}$	$P_{cal.}$
$^3F_2$	4.53	3.78	3.65	3.02	2.56	2.00
$^3F_3$	6.88	5.98	5.86	5.01	4.75	3.10
$^3F_4$	4.35	3.76	3.44	3.14	0.28	1.44
$^1G_4$	0.43	0.31	0.38	0.26	2.39	0.14
$^1D_2$	2.39	1.07	1.85	0.89	1.55	0.50
$^3P_0$	4.58	1.38	3.68	1.22	2.59	2.20
$^3P_1$	4.79	2.47	3.88	2.15	2.74	3.11
$^3P_2$	12.68	3.54	11.73	2.97	10.54	1.60
R.m.s.deviation	3.5805		3.3150		3.3675	

Computed values of Slater-Condon, Lande′, Racah, nephelauexetic ratio and bonding parameter for Pr^{3+} doped ZLCMTBB glass specimens are given in **Table 3**.

Table3. Computed values of Slater-Condon, Lande′, Racah, nephelauexetic ratio and bonding parameter for Pr^{3+} doped ZLCMTBB glass specimens.

Parameter	Free ion	ZLCMTBB PR01	ZLCMTBB PR1.5	ZLCMTBB PR02
$F_2(cm^{-1})$	322.09	300.00	300.04	299.99
$F_4(cm^{-1})$	44.46	44.26	44.28	44.25
$F_6(cm^{-1})$	4.867	4.412	4.414	4.410
$\xi_{4f}(cm^{-1})$	741.00	858.48	858.22	858.78
$E^1(cm^{-1})$	4728.92	4450.84	4451.84	4450.03
$E^2(cm^{-1})$	24.75	22.01	22.01	22.01
$E^3(cm^{-1})$	478.10	454.72	454.74	454.69
F_4/F_2	0.13804	0.14755	0.14758	0.14750
F_6/F_2	0.01511	0.01471	0.01471	0.01470
E^1/E^3	9.8911	9.7882	9.7899	9.7870
E^2/E^3	0.0518	0.0484	0.0484	0.484
β'		0.8886	0.8888	0.8885
$b^{1/2}$		0.2360	0.2357	0.2362

The values of Judd-Ofelt intensity parameters are given in **Table 4**.

Table 4. Judd-Ofelt intensity parameters for Pr^{3+} doped ZLCMTBB glass specimens.

Glass Specimen	$\Omega_2(pm^2)$	$\Omega_4(pm^2)$	$\Omega_6(pm^2)$	Ω_4/Ω_6	**References**
ZLCMTBB (PR01)	2.793	1.949	5.347	0.365	P.W.
ZLCMTBB (PR1.5)	2.114	1.724	4.460	0.387	P.W.
ZLCMTBB (PR02)	5.960	3.097	1.813	1.708	P.W.
TWPL(PR)	2.087	1.591	3.780	0.421	[24]
BPZL(PR)	8.06	6.13	9.79	0.626	[25]
ZTFB(PR)	4.620	3.275	8.632	0.379	[26]

4.5 Excitation Spectrum

Excitation spectra of ZLCMTBB PR (01) glass recorded at the emission wavelength 395 nm is depicted as figure 5. The excitation spectra consists of three peaks corresponding to the transitions from the ground state $^3H_4$ to the various excited states $^3P_2$, $^3P_1$ and $^3P_0$ at the wavelengths of 448, 465 and 486 nm respectively. Among these, a prominent excitation band at 448 nm has been selected for the measurement of emission spectrum of Pr^{3+} glass.

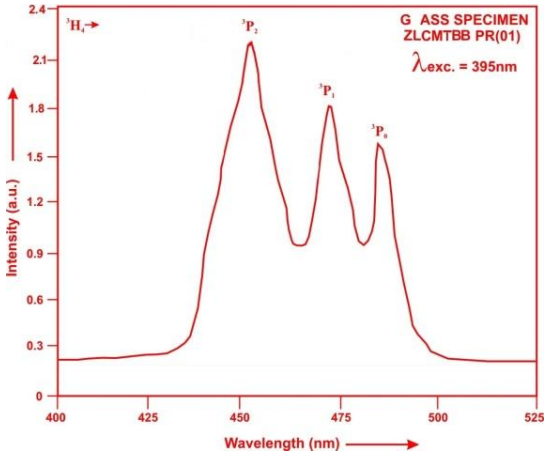

Fig.5: Excitation Spectrum of ZLCMTBB PR (01) glass.

4.6 Fluorescence Spectrum

The fluorescence spectrum of Pr^{3+}doped in Zinc lithium calcium magnesium tantalum bismuth borate glass is shown in Figure 6. There are nine broad bands ($^3P_0 \rightarrow {}^3H_4$), ($^3P_0 \rightarrow {}^3H_5$), ($^1D_2 \rightarrow {}^3H_4$) ($^3P_0 \rightarrow {}^3H_6$), ($^3P_0 \rightarrow {}^3F_2$), ($^3P_1 \rightarrow {}^3F_3$), ($^1D_2 \rightarrow {}^3H_5$), ($^3P_0 \rightarrow {}^3F_4$) and ($^1G_4 \rightarrow {}^3H_5$) respectively for glass specimens.

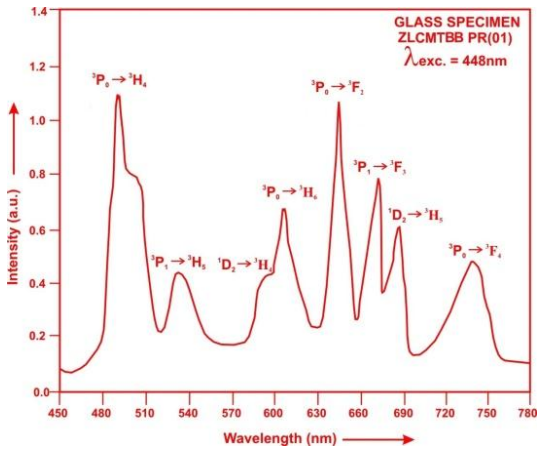

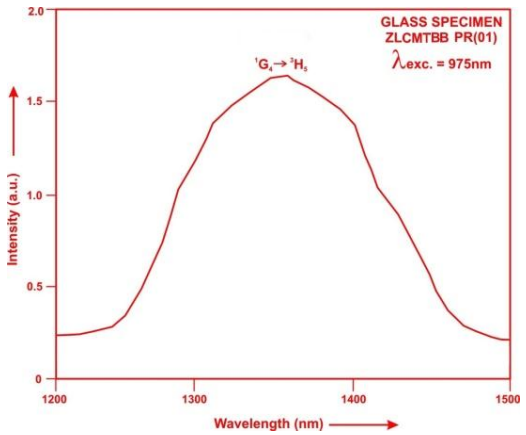

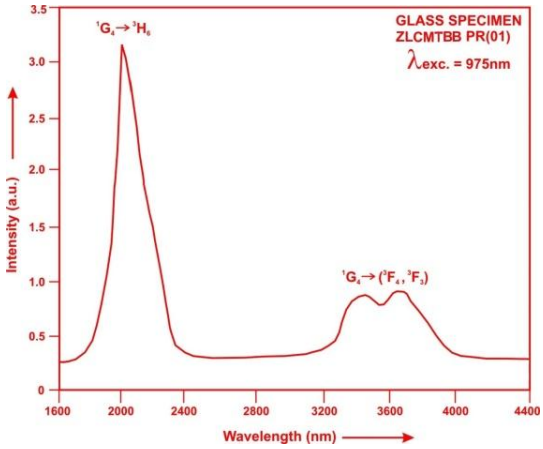

Fig.6: Fluorescence spectrum of ZLCMTBB PR (01) glass.

Table 5. Emission peak wave lengths (λ_p), radiative transition probability (A_{rad}), branching ratio (β_R), stimulated emission crosssection (σ_p), and radiative life time (τ) for various transitions in Pr^{3+} doped ZLCMTBB glasses.

Transition		ZLCMTBB PR (01)				ZLCMTBB PR (1.5)				ZLCMTBB (PR 02)			
	λ_{max} (nm)	$A_{rad}(s^{-1})$	β	σ_p (10^{-20} cm^2)	$\tau_R(\mu s)$	$A_{rad}(s^{-1})$	β	$\sigma_p(10^{-20}$ cm^2)	τ_R (μs)	$A_{rad}(s^{-1})$	β	σ_p (10^{-20} cm^2)	τ_R (10^{-20} cm^2)
$^3P_0 \rightarrow {}^3H_4$	485	1199.79	0.1099	0.406		1063.35	0.1194	0.381		1912.76	0.1113	0.780	
$^3P_1 \rightarrow {}^3H_5$	532	2303.50	0.2110	0.443		1987.85	0.2233	0.405		2341.27	0.1362	0.510	
$^1D_2 \rightarrow {}^3H_4$	599	574.56	0.0526	0.217		482.70	0.0542	0.194		291.85	0.0170	0.126	
$^3P_0 \rightarrow {}^3H_6$	602	505.03	0.0463	0.263		422.08	0.0474	0.247		171.91	0.0099	0.111	
$^3P_0 \rightarrow {}^3F_2$	643	2280.95	0.2089	2.111	126.90	1728.99	0.1942	1.886	112.311	4886.34	0.2842	6.367	58.163
$^3P_1 \rightarrow {}^3F_3$	676	337.64	0.3092	1.764		2644.07	0.2970	1.439		6875.66	0.3999	3.954	
$^1D_2 \rightarrow {}^3H_5$	685	6.094	0.0006	0.0065		5.290	0.0006	0.0065		6.922	0.0004	0.0096	
$^3P_0 \rightarrow {}^3F_4$	730	221.63	0.0230	0.1603		196.43	0.0221	0.1518		353.55	0.0206	0.290	
$^1G_4 \rightarrow {}^3H_5$	1350	274.46	0.0251	0.8686		229.44	0.0258	0.7435		138.33	0.0080	0.460	
$^1G_4 \rightarrow {}^3H_6$	2025	156.80	0.0144	5.423		127.84	0.0144	4.687		175.23	0.0102	6.725	
$^1G_4 \rightarrow ({}^3F_4, {}^3F_2)$	3555	20.04	0.0018	4.432		15.81	0.0018	3.621		39.19	0.0023	9.301	

V. Conclusion

In the present study, the glass samples of composition (35-x):Bi_2O_3:10ZnO:10Li_2O:10CaO:10MgO:10Ta_2O_5:15B_2O_3:xPr_2O_3 (where x =1, 1.5, 2 mol %) have been prepared by melt-quenching method. The stimulated emission cross-section (σ_p) has highest value for the transition ($^1G_4 \rightarrow {}^3H_6$) in all the glass specimen doped with Pr^{3+}ion. This shows that ($^1G_4 \rightarrow {}^3H_6$) transition is most probable transition and it useful for laser action.

References

[1]. Meena,S.L.(2024).Photoluminescence and Raman analysis of Nd^{3+} doped in ytterbium zinc lithium sodium barium calcium aluminophosphate glasses,IOSR,Appl.Phys.16,28-34.

[2]. Kashif,I.,Ratep,A.(2023).Luminescence in Er^{3+} co-doped bismuth germinate glass-ceramics for blue and green emitting applications, J.Korean Ceram.Soci.60,511-526.

[3]. Bardins,M.,Vakula,N.,Petit,L(2025).Emission efficiency at 1 μm from low Yb^{3+} concentrated tellurite glass-ceramics:Alternative materiala for the future rare- earth metal shortage,255,116355.

[4]. X. Li, Z. Guan, Y. Duan, R. Shen, Y. Tian, X. Wang, S. Xu, H. Yu, X. Zhang and B. Chen, Bright green up-conversion luminescence of LaNbO4: Nd^{3+}/Yb^{3+}/Ho^{3+} phosphors under 808 nm and 980 nm excitations and the effects of dopant concentration, J. Lumin., 2022, 241, 118524.

[5]. Matos,I.M.,Balzaretti,N.M.(2024).Effect of mixed alkali ions on the structural and spectroscopic properties of Nd^{3+} doped silicate glasses, Results Mat.21,100517.

[6]. Mohan,S.,Kaur,S.,Singh,D.P.,Kaur,Puneet(2017).Structural and luminescence properties of samarium doped lead alumina borate glasses.Opt.Mat.73,223-233.

[7]. Hussein,E.M.A.,Galil,A.A.(2023).Synthesis,optical,chemical and electrical characterizations of γ-irradiated transition metal ions reinforced borate glass,J.Non.Cryst.Solids,610,122302.

[8]. Zakaly,H.M.,Abouhaswa,A.S.,Issa,S.A.M.,Mostafa,M.Y.A.,Pyshkina,M.,Optical and nuclear radiation shielding properties of zinc borate glasses doped with lanthanum oxide,J.Lumin.543,120151(2020).

[9]. Meena,S.L.(2024).Structural,Physical and Optical properties of Pr^{3+} doped in bismuth borate glasses,Appl.Phys.A,404,1-12.

[10]. Kolavekar,S.B.,Ayachit,N.H.(2021).Impact of Pr_2O_3 on the physical and optical properties of multi-component borate glasses,Mat.Chem.Phys.257,123796.

[11]. Elkhoshkhany,N.,Samir,N.,Yousef,EL S.(2020).Structural,thermal and optical properties of oxy-fluoro borotellurite glasses,Mat.Tech.9,2946-2959.

[12]. Kaur,R.,Rakesh,R.B.,Mhatre,S.,Bhatia,V.,Kumar,D.,Singh,H.Singh,S.P.Kumar,Ashok(2021).Physical,optical,structural and thermolunescence behaviour of borosilicate glasses doped with trivalent neodymium ions,Opt.Mat.117,111109

[13]. Sailaja,P.,Mahamuda,Sk.,Dedeepya,G.,Alzahrani,J.S.,Swapna,K.,Venkateswarlu,M.,Rao,A.S.,Alrowaili,Z.A.,Olarinoya,I.O.,Al-Buriahi,M.S.(2024).Effect of Eu^{3+} ions concentration on visible red luminescence and radiative shielding properties of SrO-Al_2O_3-$BaCl_2$-B_2O_3-TeO_2 glasses,Rad.Phys.Chem.216,111467.

[14]. Fang,T.,Guoxing,X.,Yuqin,M.,Yunlong,Z.,Binhao,G.,Shunfa,C.,Dexiao,C.,Yumeng,B.,Dechun,Z.(2024).Structure and Spectral properties of Er^{3+} doped bismuth borate tellurite near-infrared laser glasses,Mat.17,3292.

[15]. Mahlovanyi,B.,Truax,M.,Luchechko,A.,Shpotyuk,Y.,Yang,G.,Golovchak,R.,Kovalskiy,A.,Cebulski,J.(2023).Optical properties and tunable luminescence of Ce^{3+}/Dy^{3+} doped lithium borate glasses for photonic applications.

[16]. Lakshmi,Y.A.,Swapna,K.,Mahamuda,Sk.,Venkateswarlu,Rao,A.S.(2021).Photoluminescence properties of Sm^{3+} ions doped bismuth bprptellurite glasses,Solid State Sci.116,106609.

[17]. Meena, S.L. (2024).Spectral and Thermal analysis of praseodymium doped bismuth borate glasses for thermionic applications. IOSR J.Appl.Phys.16, 20-27.

[18]. Gorller-Walrand, C. and Binnemans, K. (1988). Spectral Intensities of f-f Transition. In: Gshneidner Jr., K.A. and Eyring,L., Eds., Handbook on the Physics and Chemistry of Rare Earths, Vol. 25, Chap. 167, North-Holland, Amsterdam, 101-264.

[19]. Meena,S.L.(2024).Spectral and Luminescence Study of Er^{3+} Doped Phosphate Glasses for the Development of 1.5 μm Broadband Amplifier, IOSR Appl.Phys.35-41.

[20]. Judd, B.R. (1962).Optical absorption intensities of rare earth ions, Phys.Rev.127, 750-761.

[21]. Ofelt,G.S. (1962). Intensities of crystal spectra of rare earth Ions, Chem.Phys37, 511-520.

[22]. Sinha, S.P. (1983). Systematics and properties of lanthanides, Reidel, Dordrecht.

[23]. Krupke, W.F. (1974).IEEE J. Quantum Electron QE, 10,450

[24]. Burtan,B.,Cisowski,J.,Mazurak,Z.,Jarzabek,B.,Czaja,M.,Reben,M.,Grelowska,I.(2014).Concentration-dependent spectroscopic properties of Pr^{3+} ions in TeO_2-WO_3-PbO-La_2O_3 glass, J.Non-Cryst.Solids 400,21-26.

[25]. Srivastava, P., Rai, S.B., Rai,D.K.(2004). Effect of lead oxide on optical properties of Pr^{3+} doped some borate based glasses, J.Alloy.Compd.368, 1-7.

[26]. Suthanthirakumar, P.,Basavapoornima,Ch.,Marimuthu,K.(2017).Effect of Pr^{3+} ions concentration on the spectroscopic properties of zinc telluro-fluoroborate glasses for laser and optical amplifier,J.Lumin.187,392-402.